PNAS RESEARCH ARTICLE | CHEMISTRY NEUROSCIENCE

Nanoelectrochemistry reveals how soluble $A\beta_{42}$ oligomers alter vesicular storage and release of glutamate

Xiao-Ke Yang[a], Fu-Li Zhang[a], Xue-Ke Jin[a], Yu-Ting Jiao[a], Xin-Wei Zhang[a], Yan-Ling Liu[a], Christian Amatore[b,c,1], and Wei-Hua Huang[a,d,1]

Edited by Catherine Murphy, University of Illinois at Urbana-Champaign, Urbana, IL; received November 23, 2022; accepted March 30, 2023

Glutamate (Glu) is the major excitatory transmitter in the nervous system. Impairment of its vesicular release by β-amyloid (Aβ) oligomers is thought to participate in pathological processes leading to Alzheimer's disease. However, it remains unclear whether soluble $A\beta_{42}$ oligomers affect intravesicular amounts of Glu or their release in the brain, or both. Measurements made in this work on single Glu varicosities with an amperometric nanowire Glu biosensor revealed that soluble $A\beta_{42}$ oligomers first caused a dramatic increase in vesicular Glu storage and stimulation-induced release, accompanied by a high level of parallel spontaneous exocytosis, ultimately resulting in the depletion of intravesicular Glu content and greatly reduced release. Molecular biology tools and mouse models of Aβ amyloidosis have further established that the transient hyperexcitation observed during the primary pathological stage is mediated by an altered behavior of VGLUT1 responsible for transporting Glu into synaptic vesicles. Thereafter, an overexpression of Vps10p-tail-interactor-1a, a protein that maintains spontaneous release of neurotransmitters by selective interaction with t-SNAREs, resulted in a depletion of intravesicular Glu content, triggering advanced-stage neuronal malfunction. These findings are expected to open perspectives for remediating $A\beta_{42}$-induced neuronal hyperactivity and neuronal degeneration.

soluble $A\beta_{42}$ oligomers | vesicular glutamate storage | stimulation-induced release | spontaneous exocytosis | release fraction

Significance

Neurotransmission in the brain relies on synaptic vesicles which store neurotransmitters and release them to transfer information between neurons. Therefore, any alteration of these functions critically alters brain behavior. β-amyloid oligomers (Aβ) are suspected to be severely involved in Alzheimer's disease (AD) although the mechanism remains highly debated. Our nanoelectrochemical results make an important contribution to this debate by providing direct quantitative and kinetic in situ evidences that soluble $A\beta_{42}$oligomers significantly increase intravesicular Glu storage and its vesicular release from Glu-containing vesicles present in varicosities. Coupled with other biological investigations, including with AD mouse models, these data revealed that soluble $A\beta_{42}$oligomers modify the Glu pathway by altering the behavior of two proteins controlling Glu loading and spontaneous exocytosis.

Alzheimer's disease (AD) is a neurodegenerative disease associated with the accumulation of pathogenic amyloid-β (Aβ) in the brain that causes synaptic dysfunction and inflammation, leading to the ultimate death of neurons with severe consequences on the patients' cognitive ability (1–3). Extensive evidence points to continued Aβ-dependent impairment at both inhibitory and excitatory synapses (4–6). Specifically, impaired glutamate (Glu) homeostasis is evident in both AD patients and animal models and may disrupt the strength and plasticity of glutamatergic synaptic transmission (7–10). Glu is the most important primary excitatory neurotransmitter released by vesicular exocytosis in the central nervous system. Any fine modulation of its intravesicular Glu content and/or its released quantities plays a particularly crucial role in major brain functions such as cognition, learning, and memory, as well as many neurological disorders (11).

Previous studies through chromatographic analysis, optics, electrophysiology, and molecular biological tools suggested that $A\beta_{1\text{-}42}$ (i.e., the 42 amino acid form of amyloid β and further named $A\beta_{42}$ for simplification) and/or their oligomers preferentially impair the homeostasis of extracellular Glu and cause early neuronal hyperactivity by blocking Glu reuptake (12–14) or enhancing Glu release probability (15). Other studies proposed that $A\beta_{42}$ acts by modulating vesicular Glu release through altering vesicle synthesis and loading processes, or by interfering with protein–protein interactions (16–18), leading to dysfunction of synaptic transmission. It is, therefore, essential to be able to quantitatively determine the content of Glu vesicles and to precisely record their exocytosis regimes, if possible in single living neurons, in order to better understand the mechanism of $A\beta_{42}$-induced synaptic damage in AD.

Due to its high sensitivity, selectivity, and excellent spatio-temporal resolution, direct amperometric electrochemistry at micro/nanoelectrodes has offered a panel of powerful tools to neurosciences, allowing the quantification of important electroactive molecules such as dopamine, norepinephrine, and epinephrine, stored in individual vesicles and for precisely monitoring their transient exocytotic releasing events (19–26). Since Glu molecules are not electroactive, their direct faradic detection is impossible. However, through modification of Pt-based microelectrode surfaces with glutamate oxidase (GluOx), vesicular Glu content and exocytotic release could be determined in brain slices, cultured neurons (27–30), or isolated vesicles (31). Such GluOx-modified cylindrical nanoelectrodes allowed recording quantitative proofs that $A\beta_{42}$ led to anomalous release of Glu molecules by neuronal varicosities during elicited vesicular exocytosis relative to

Author contributions: X.-K.Y. and W.-H.H. designed research; X.-K.Y. performed research; X.-K.J., Y.-T.J., X.-W.Z., and Y.-L.L. contributed new reagents/analytic tools; X.-K.Y., F.-L.Z., and W.-H.H. analyzed data; and X.-K.Y., C.A., and W.-H.H. wrote the paper.

The authors declare no competing interest.

This article is a PNAS Direct Submission.

[1]To whom correspondence may be addressed. Email: christian.amatore@ens.psl.eu or whhuang@whu.edu.cn.

This article contains supporting information online at https://www.pnas.org/lookup/suppl/doi:10.1073/pnas.2219994120/-/DCSupplemental.

Published May 1, 2023.

control (30). However, it was then impossible to decide whether this was due to induced changes in the number of Glu molecules stored in the vesicles or evidenced differences between the released fractions since both factors influence the released amounts (24). We recently developed a nanowire Glu biosensor with high sensitivity and selectivity, good spatio-temporal resolution, and superior mechanical toughness that enabled measurements of intravesicular Glu content inside individual vesicles of varicosities of living neurons as well as Glu-released quantities (32). This prompted us to apply this Glu nanosensor to address this crucial question by unravelling the action of $A\beta_{42}$ on factors controlling Glu release from varicosities of living murine hippocampal neurons, as shown below.

Our data established that short-duration incubations of the living neurons with $A\beta_{42}$ induced a dramatic increase in vesicular Glu storage and in magnitudes of K^+-evoked release spikes. Conversely, continuous incubation with $A\beta_{42}$ evoked large series of spontaneous exocytotic events that progressively and irreversibly decreased the intravesicular Glu content as well as the amounts released. Further analysis of the Glu spikes indicated that $A\beta_{42}$ treatment increased the released Glu fractions possibly by enlarging the fusion pore. Other specific biological experiments carried out on neurons and AD mouse models (APP/PS1) suggested that the alteration and disorder of Glu storage and of the release events characteristics induced by $A\beta_{42}$ were mainly mediated by two proteins. Expression of VGLUT1 (vesicular Glu transporter 1) which associates with synaptic vesicle (SV) membranes to enable vesicular Glu storage was found to be significantly down-regulated by $A\beta_{42}$, which is likely the cause of lower intravesicular storage. In contrast, $A\beta_{42}$ induced an increase in Vps10p-tail-interactor-1a (Vti1a), a protein that mediates fusion pore formation and stability due to its interactions with t-SNAREs, which is expected to favor the occurrence of high-frequency spontaneous exocytotic events (22, 33).

Altogether, this body of evidence presenting quantitative data related to $A\beta_{42}$-induced changes in intravesicular Glu storage and exocytotic events characteristics revealed by our unique Glu-sensitive electrochemical nanosensor while contrasting them with the observation of opposing biological effects of $A\beta_{42}$ on two key proteins, VGLUT1 and Vti1a, provides a critical understanding of the Glu-related mechanisms associated with the development of AD.

Results and Discussion

Detection of $A\beta_{42}$-Regulated Glu Release from Hippocampal Neurons. To investigate the different effects of soluble $A\beta_{42}$ oligomers on Glu vesicular exocytosis, hippocampal neurons were incubated with $A\beta_{42}$ oligomers for 15, 30, 180, and 300 min to simulate in vitro, respectively, early and late stages of AD according to MTT assay (*SI Appendix*, Fig. S1) and previous publication (30, 34, 35). A cylindrical nanowire Glu bioelectrochemical sensor with excellent performance toward Glu detection (*SI Appendix*, Fig. S2) was used to quantify the vesicular Glu release from varicosity in hippocampal neuron, as shown in Fig. 1*A*. To ensure a reproductible distance between the cell membrane and the nanoelectrode, the cylindrical surface of the Glu sensor was approached close to the varicosity until a gentle deformation of its membrane was observed. Sequences of well-defined amperometric spikes were then recorded from Glu-containing neuronal varicosities stimulated by high-K^+ solution (62.5 mM) local puffs under all circumstances investigated in this work, viz., without $A\beta_{42}$ (controls) and after short and long incubations with $A\beta_{42}$ (Fig. 1*B*). Each of these spikes represents the 2-electron oxidation

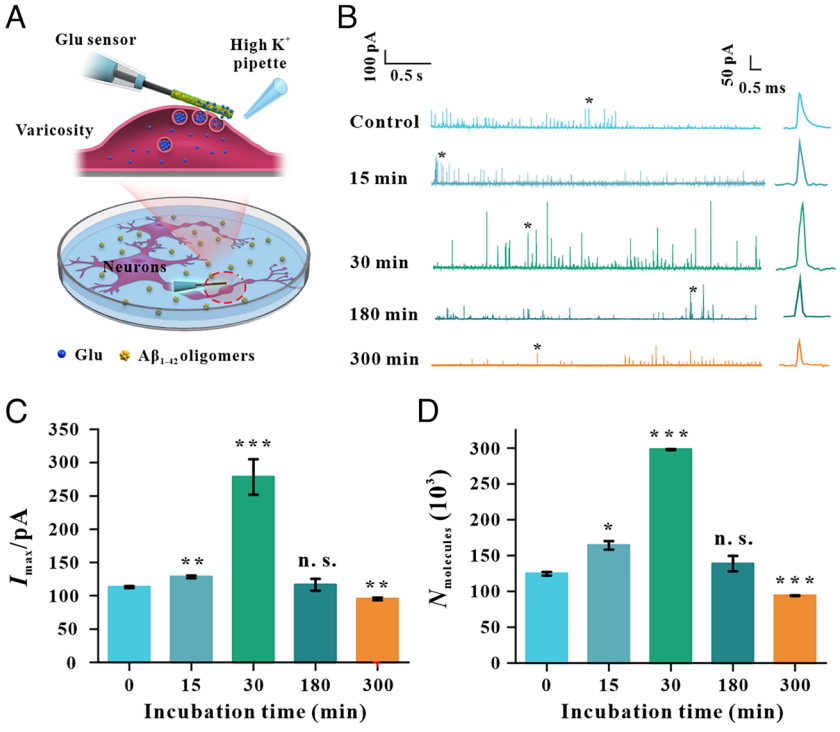

Fig. 1. Detection of $A\beta_{42}$-regulated Glu release from hippocampal neurons. (*A*) Schematic diagram showing the process of amperometric monitoring of Glu exocytosis from single hippocampal varicosity incubated with 250 nM $A\beta_{42}$ oligomers. (*B*) Amperometric traces from Glu sensor placed on varicosities with applied potential at 700 mV (vs. Ag/AgCl reference electrode). Comparison of (*C*) I_{max} and (*D*) the numbers of Glu molecules released during vesicular exocytotic events (n = 351 events from 15 normal neurons, n = 363 events from 10 neurons with 15 min $A\beta_{42}$ oligomer treatment, n = 459 events from 11 neurons with 30 min $A\beta_{42}$ treatment, n = 267 events from 12 neurons with 180 min $A\beta_{42}$ oligomer treatment, n = 524 events from 26 neurons with 300 min $A\beta_{42}$ oligomer treatment). Error is SEM, ***$P < 0.001$, n. s.: no significance compared with control.

current of Glu released through exocytosis by a single vesicle (27, 29, 32). Then, series of individual releasing flux intensities featured by each spike peak current (I_{max}) and number of released molecules (N) given by their electrical charges (Q) can be readily determined with high accuracy and precision. Based on the analysis of electrochemical data (Fig. 1 *C* and *D* and *SI Appendix*, Table S1), the released fluxes evidenced by I_{max} values and intravesicular content (N) first increased upon increasing the incubation times (15 and 30 min) and then decreased (180 and 300 min). The changes and figures observed for 30 and 300 min treatment with $A\beta_{42}$ oligomers represent cells experiencing no damage and severe damage, respectively. On the contrary, the maximum of release quantities was observed after 30 min incubation with $A\beta_{42}$ oligomers, while 300 min incubation times featured the lowest ones over the range of incubation times investigated. Therefore, we selected 0, 30, and 300 min as perfectly representative of the cells' evolution with incubation times with $A\beta_{42}$ oligomers. According to Faraday's law, $Q = 2FN$ *and* $I_{max} = 2F(dN/dt)_{max}$ where $F = 96{,}500$ C is the Faraday constant. Statistical analyses of these data evidenced that the average I_{max} and N were 113.1 ± 15.3 pA and 125,000 ± 3,000 molecules (mean ± SEM, n = 351, 15 cells), respectively, per single exocytotic control event (Fig. 1 *C* and *D* and *SI Appendix*, Table S1). After incubation with soluble $A\beta_{42}$ oligomers for 30 min, the average I_{max} and N were calculated to be 278.5 ± 26.7 pA and 298,000 ± 4,000 molecules (n = 459, 11 cells), respectively, i.e., *ca.* 2.5 times larger than for controls. Such drastic increases revealed that short-duration $A\beta_{42}$ incubations induced significantly higher Glu releases than those in controls with presumably a higher excitability of synaptic transmission under in vivo conditions. In contrast, long-duration (300 min) incubations with soluble $A\beta_{42}$ oligomers led to a considerable reduction of Glu release (I_{max} = 95.1 ± 7.7 pA, and N = 94,000 ± 500 molecules, n = 524, 26 cells) vs. short-duration ones being, respectively, even *ca.* 20% and *ca.* 25% smaller than those for controls (Fig. 1 *C* and *D* and *SI Appendix*, Table S1). Such significant decrease of Glu-release by neuronal varicosities induced by long-time exposition to $A\beta_{42}$ is expected to impair synaptic transmission under in vivo conditions, resulting in the axonal pathologies reported in AD (36). Altogether, this set of in vitro experiments support previous in vivo observations that soluble $A\beta_{42}$ oligomers induced synaptic hyperexcitation during early stages of the disease (12), while the decrease of Glu release noted here for long-time incubations $A\beta_{42}$ is fully coherent with the synaptic dysfunction leading to the neurodegeneration observed during late stages of AD (37).

Quantitative Measurement of $A\beta_{42}$-Dependent Intravesicular Glu Content. In the previous section, we evidenced two contrasting effects induced by soluble $A\beta_{42}$ oligomers on the magnitude of Glu exocytotic release by neuronal varicosities. However, this may have two causes, viz., a change of the intravesicular Glu content or a difference on the exocytotic characteristics (22, 23), or any combination of both (22, 33, 38–40). To solve this important issue, we relied on intracellular vesicle impact electrochemical cytometry (IVIEC) using the same Glu nanosensor (32).

Upon inserting the Glu-sensing tip of the nanoelectrode into hippocampal neuronal varicosities (Fig. 2*A*), each single Glu-containing vesicle contacting the electrode surface spontaneously burst open and spilled their full content onto it where Glu was oxidized. Thus, sequences of current spikes were recorded (Fig. 2*B*) as was observed during exocytotic vesicular release (Fig. 1*B*) except that now each amperometric IVIEC spike featured the full Glu intravesicular content (32). The same statistical analyses as detailed above performed for controls provided I_{max} = 414.3 ± 6.7 pA and N = 361,000 ± 4,000 molecules per single vesicle (mean ± SEM, n = 598, 10 cells) (Fig. 2*C* and *SI Appendix*, Fig. S3). Comparison to the average N value (125,000 ± 3,000 molecules) monitored for the released Glu control quantities evidenced that only 35% of the intravesicular content was released, in agreement with our previous report (32). After incubation with soluble $A\beta_{42}$ oligomers for 15 and 30 min, the corresponding values were 406.6 ± 1.0 pA and 385,000 ± 6,000 molecules (mean ± SEM, n = 340, 5 cells) and 512.7 ± 28.2 pA and 478,000 ± 4,000 molecules (mean ± SEM, n = 451, 6 cells), indicating a significant increase in the intravesicular Glu content, i.e., by a factor *ca.* 1.1 and 1.3 vs. controls, respectively. Interestingly, the released fraction during exocytotic events constantly increased, resulted to be *ca.* 40% and 60%, respectively, suggesting that the exocytotic fusion pores were significantly enlarged (22, 33).

Long-term incubations with soluble $A\beta_{42}$ oligomers for 180 and 300 min provided I_{max} = 165.6 ± 1.1 pA and N = 205,000 ± 4,000 molecules (n = 299, 12 cells) and I_{max} = 122.3 ± 5.9 pA and N = 118,000 ± 2,000 molecules (n = 720, 32 cells) for the IVIEC spikes, respectively, i.e., intravesicular Glu content was decreased by *ca.* 45% and 65%, respectively, compared with controls (Fig. 2 *C* and *D* and *SI Appendix*, Fig. S4). Conversely, the Glu-released fraction (*ca.* 70% for 180 min and 80% for 300 min) was increased, being larger than that for controls (*ca.* 35%) and even larger than that for hippocampal neuronal varicosities pretreated with soluble $A\beta_{42}$ oligomers during short time (*ca.* 45% for 15 min and 60% for 30 min) (*SI Appendix*, Fig. S4). This suggested that long-time exposure to $A\beta_{42}$ led to an even larger expansion of the fusion pores than short-time ones in opposition with the lower relative Glu content. These contrasting data suggested that incubation with soluble $A\beta_{42}$ oligomers induced two opposite effects with different consequences revealed by the durations of the incubation time.

The significant and monotonous increase of exocytotic Glu-released fractions in the presence of $A\beta_{42}$ suggested that soluble $A\beta_{42}$ oligomers modified the vesicular exocytosis kinetics by enlarging the fusion pore size (33, 41–43). To further support this hypothesis, we further analyzed the variations of the exponential decay times of individual exocytotic spikes under each conditions. The corresponding decay time constants vary reciprocally with the radius of the exocytotic fusion pores (33) and are proportional to the time durations, t_{fall}, required for the spike currents to decrease from 0.75 I_{max} and 0.25 I_{max} as defined in Fig. 2*E* and *SI Appendix*, Fig. S5 and Table S1 shows that the t_{fall} values are *ca.* 70% and 66% for 30 min and 300 min $A\beta_{42}$ treatments, respectively, compared to controls (*SI Appendix*, Table S1), which translate in an increase of the fusion pores radii by *ca.* 45% and 50%, respectively, compared to controls (33, 41–43). This enlargement of the Glu vesicles fusion pores confirms quantitatively the previously suggested occurrence of an interaction of $A\beta_{42}$ with the synaptophysin/VAMP2 complex which is regulating the formation of the fusion pore (16), therefore modifying synaptic strength and plasticity (2, 44).

$A\beta_{42}$ Oligomers Modify VGLUT1 Expression Level in Vesicles. We sought for a heuristic explanation for the observed increase of intravesicular Glu content at short-duration incubation times of hippocampal neurons with $A\beta_{42}$. At glutamatergic synapses, loading of Glu into SVs is mainly achieved by VGLUT1, so the intravesicular Glu content depends on VGLUT1 expression level (45–47). Immunofluorescence results in Fig. 3*A* confirmed that hippocampal neurons incubated with soluble $A\beta_{42}$ oligomers during 30 min exhibited an obvious increase in VGLUT1 levels compared to control (Fig. 3*B*), which is consistent with the

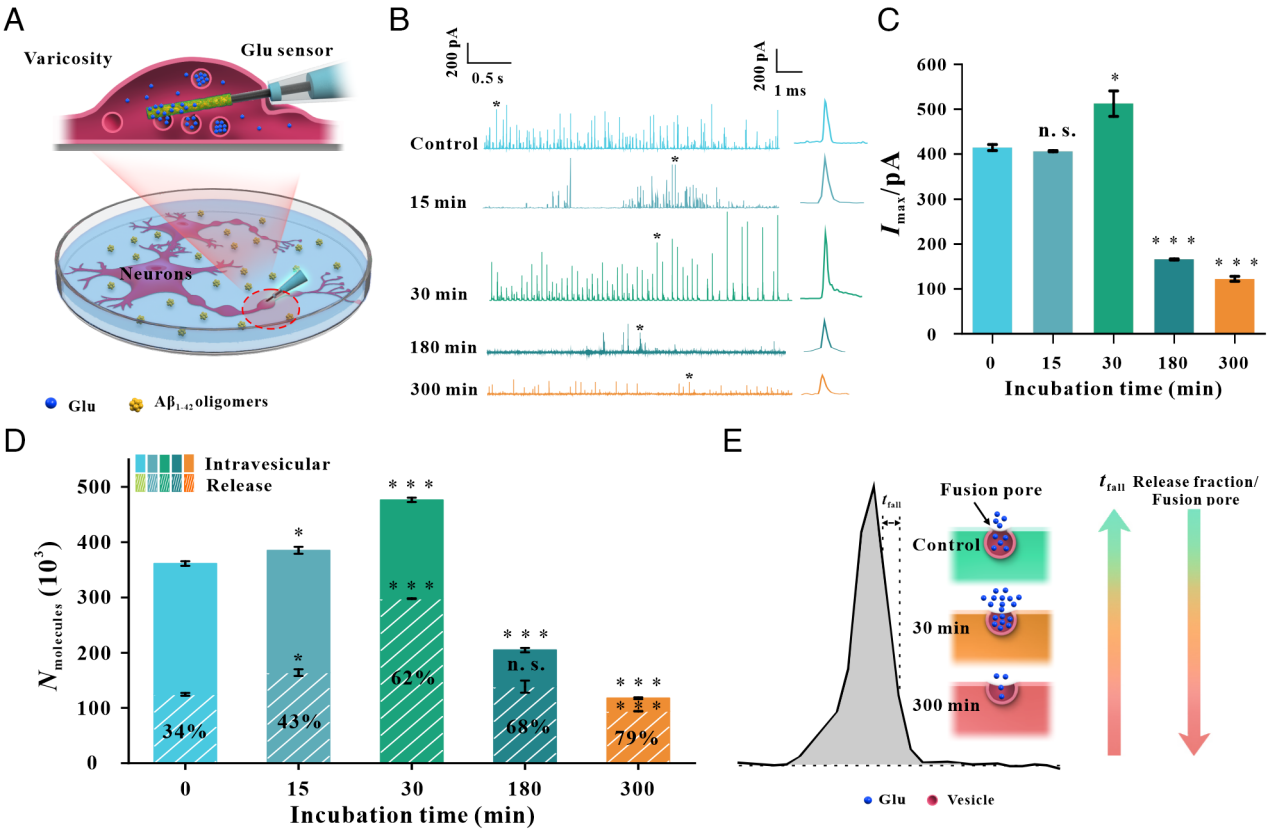

Fig. 2. Measurement of $A\beta_{42}$-regulated intravesicular Glu content and its release fraction. (*A*) Schematic cartoon showing the IVIEC process for amperometric monitoring of the intracellular Glu content of vesicles from single hippocampal varicosity treated with soluble $A\beta_{42}$ oligomers. (*B*) Amperometric traces from Glu sensor placed inside a varicosity untreated (control) or treated with 250 nM $A\beta_{42}$ oligomers (30 or 300 min) at 700 mV (vs. Ag/AgCl reference electrode). Comparison of (*C*) I_{max} and (*D*) the mean numbers of Glu molecules stored in the intracellular vesicle and released during vesicular exocytotic events (IVIEC measurements: n = 598 events from 10 untreated neurons, n = 340 events from 5 neurons with 15 min $A\beta_{42}$ oligomer treatment, n = 451 events from 6 neurons with 30 min $A\beta_{42}$ oligomer treatment, n = 299 events from 12 neurons with 180 min $A\beta_{42}$ oligomer treatment, n = 720 events from 32 neurons with 300 min $A\beta_{42}$ oligomer treatment). (*E*) Schematic diagram rationalizing the observed dual influence of soluble $A\beta_{42}$ oligomers on Glu vesicular release. Error is SEM, $^{*}P < 0.05$, $^{***}P < 0.001$, compared with control.

corresponding increase in Glu intravesicular quantities (Fig. 1*D*). To better correlate in vitro results with in vivo conditions of AD, the amount of VGLUT1 in APP/PS1 (APPSWE, PSEN1dE9) transgenic mouse models (*SI Appendix*, Fig. S6) which are assumed to feature AD progression in patients (*SI Appendix*, Fig. S7) was quantified by western blot assay. As shown in Fig. 3 *C* and *D*, the amount of VGLUT1 at the early stage of AD mice (2-mo-old APP/PS1 mice) (48) was found to be significantly higher than that of 2-mo-old wild-type (WT) mice being consistent with the immunofluorescence data (Fig. 3*B*). This suggests the existence of a causative correlation between the overexpression of VGLUT1 and the increase of Glu loading of varicosity vesicles during the short-time treatment with soluble $A\beta_{42}$ oligomers.

In contrast, 7-mo APP/PS1 mice experienced a dramatic depletion of their VGLUT1 level compared to age-matched control mice (Fig. 3*D*) in agreement with the VGLUT1 decrease shown by the decrease of immunofluorescence levels in AD cell models after 300 min incubation compared with control cells (Fig. 3*B*). This suggests that at the later stage of AD, $A\beta_{42}$ oligomers may down-regulate the expression of VGLUT1, hence impairing vesicle replenishment or rapid reloading of empty recycled vesicle, resulting in an overall significant decrease of the average intravesicular Glu content.

$A\beta_{42}$ Oligomers Induce Spontaneous High-Frequency Glu Exocytosis. In the central nervous system, apart from evoked release, synapses may also spontaneously release neurotransmitter quantities at a low frequency (49). Additionally, previous studies performed on rodent hippocampal cell cultures indicated that neurons placed under AD conditions may increase their spontaneous release probability and intrinsic excitability, leading to pathological effect on synaptic transmission in vivo and in vitro (15, 50).

This prompted us to investigate with our Glu nanosensor whether a similar behavior was occurring in our hippocampal neuron models when exposed to $A\beta_{42}$ oligomers. At single varicosities of untreated hippocampal neurons, in the absence of K^+-stimulation and without $A\beta_{42}$, as expected, only rare spikes of small amplitudes (i.e., with I_{max} less *ca.* 50 pA) could be observed per minute (Fig. 4*A*). In contrast, when the cultured hippocampal neurons were preincubated with $A\beta_{42}$ oligomers during 30 min, and investigated again without K^+-stimulation, both the frequency and the mean amplitude of the amperometric spikes were significantly increased (Fig. 4*A* and *SI Appendix*, Table S2). Statistical analyses showed that (7 ± 2) spikes per minute (mean ± SEM) were recorded from control groups (no K^+, no $A\beta_{42}$), while this frequency increased by *ca.* 142% (17 ± 5) spikes per minute (mean ± SEM) after treating the neurons with $A\beta_{42}$ oligomers for 30 min still without K^+-stimulation. Peak currents (I_{max}) increased by *ca.* 16% (58.8 ± 1.2 pA) vs. control (50.7 ± 1.8 pA) (Fig. 4*B*). These values were *ca.* twice smaller in the absence of $A\beta_{42}$ treatment and *ca.* 20% lower after 30 min $A\beta_{42}$ incubation compared to those observed under the same conditions with K^+-stimulation. This indicated that the spontaneous fusion pores were much smaller than those evoked by K^+ stimulation in agreement with expected

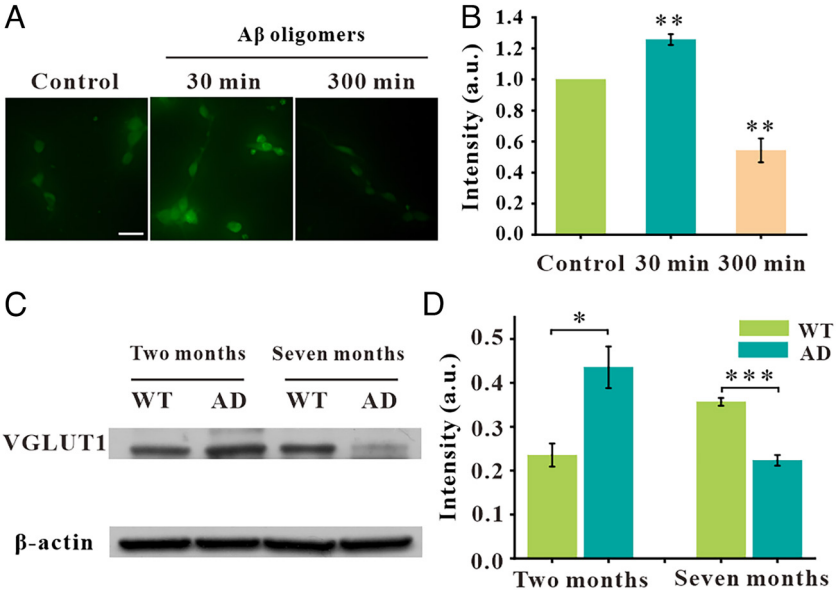

Fig. 3. Influence of $A\beta_{42}$ oligomers on the VGLUT1 expression level in intracellular Glu vesicles. (*A*) Representative immunofluorescence images of VGLUT1 levels in cultured hippocampal neurons exposed to control conditions or incubated with 250 nM $A\beta_{42}$ soluble oligomers during 30 or 300 min. (Common scale bar: 60 μm.) (*B*) Integrated VGLUT1 immunofluorescence levels. (*C*) Western blots of hippocampal tissues from 2- or 7-mo-old wild-type (WT) and APP/PSI mice (AD), respectively. β-actin was used as a density control. (*D*) Histograms of density analysis for VGLUT1 level. Error is SEM; $^*P < 0.05$, $^{**}P < 0.01$, $^{***}P < 0.001$, compared with control.

transient pores in bilipid membranes. More interesting is the fact that the spikes exhibited larger time characteristics $t_{1/2}$, $t_{rise,}$ and t_{fall} (see definitions in *SI Appendix*, Fig. S5), which increased by *ca.* 15%, 40%, and 35%, respectively (Fig. 4*C*), indicating that $A\beta_{42}$ oligomers induced a long-lasting spontaneous fusion pores. This was coherent with the *ca.* 60% increase of the average Glu quantities released through such spontaneous pores after 30 min incubation with $A\beta_{42}$, i.e., 52,000 ± 700 molecules per spike (n = 191, 10 cells) vs. 31,000 ± 400 molecules per spike (n = 211, 25 cells) without incubation (Fig. 4*D*). This revealed that soluble $A\beta_{42}$ oligomers played a crucial role through promoting spontaneous release of Glu which might contribute to the primary pathology leading to neuron hyperactivity in early AD. For the 300 min $A\beta_{42}$ oligomers-treated group, only very few spontaneous spikes were detected from 30 neurons. This phenomenon might be due to the fact that 300 min incubations caused significant cell damage and severe neurite atrophy (see the MTT test in *SI Appendix*, Fig. S1).

$A\beta_{42}$ Oligomers Modify Vti1a Expression Level on Vesicles. Our data strongly suggest that the capacity of soluble $A\beta_{42}$ oligomers

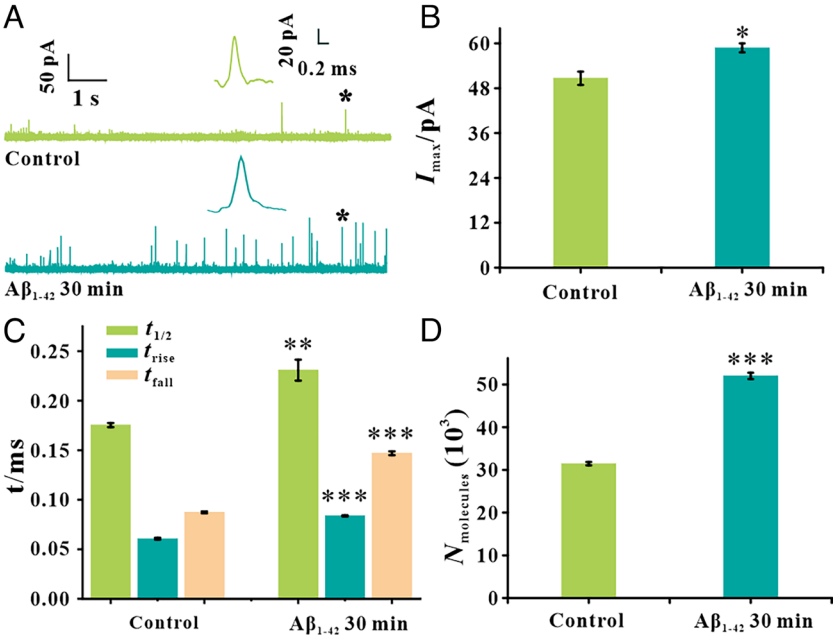

Fig. 4. Amperometric measurement of spontaneous Glu exocytosis in controls or after 30 min incubation with $A\beta_{42}$ soluble oligomers. (*A*) Typical amperometric traces recorded by Glu nanosensors placed on varicosities without any high-K^+ stimulation. A potential at 700 mV (vs. Ag/AgCl reference electrode) was applied (control n = 211 events from 25 untreated neurons; n = 191 events from 10 neurons incubated with $A\beta_{42}$ oligomers during 30 min). Comparison of (*B*) I_{max}, (*C*) $t_{1/2}t_{rise}$, and t_{fall}, and (*D*) $N_{molecule}$, of exocytotic spikes for control hippocampal neurons or after 30 min incubation with $A\beta_{42}$ soluble oligomers. Error is SEM; $^*P < 0.05$, $^{**}P < 0.01$, $^{***}P < 0.001$, compared with control.

promoted spontaneous Glu release, which may participate, at least in part, in the regulation of the vesicular Glu content from early to late stages of AD cell models. However, the relationship between $A\beta_{42}$ and the change of the characteristics of spontaneous release of Glu remains unclear. This is an important issue since "normal" spontaneous Glu release mediated by synaptic membrane fusion machinery has important biological function in brain (51). Recent studies indicated that spontaneous neurotransmitter vesicular release is mediated by Vti1a, a protein associated with SVs (51–53). Gain and loss of Vti1a function result in up- and downregulation of the frequency of spontaneous events, respectively (54). Therefore, the level of Vti1a was quantified in vitro and in vivo by immunofluorescence imaging and western blot assay. This evidenced that after being treated with $A\beta_{42}$ oligomers for 30 min (Fig. 5 *A*–*D*), neurons exhibited an obvious increase in Vti1a levels compared to controls. A same outcome was observed upon comparing 2-mo-old APP/PS1 mice to age-matched control mice. Both of these in vivo and in vitro results were fully coherent with the trend of the amperometric observations reported in Fig. 4.

All these results concur to suggest that $A\beta_{42}$-soluble oligomers up-regulated Vti1a expression, resulting in a drastic increase of the spontaneous frequency of Glu-release vesicular activity. Combined with the downexpression of VGLUT1 induced by long exposition to $A\beta_{42}$-soluble oligomers, this increased spontaneous release provides a tentative justification for the observation of lowest intravesicular Glu contents at late AD stages as sketched in Fig. 5*G* and therefore to synaptic dysfunction/loss which exacerbates the disease course.

Conclusion

Thanks to our cylindrical nanowire Glu sensor, the variations of intravesicular Glu contents and of Glu-released fractions at single hippocampal neuron varicosities induced by short (30 min) and long (300 min) incubations with $A\beta_{42}$ soluble oligomers could be determined with significative precision. Combined with molecular biological tools and AD mouse models, these bioelectrochemical results strongly establish that: i) soluble $A\beta_{42}$ oligomers up-regulate the expression of VGLUT1 at early stage of AD, promoting a dramatic increase in both vesicular Glu content and vesicular release, presumably being one of the physiologic causes of neuronal hyperexcitation; ii) in contrast, as the disease progresses, $A\beta_{42}$ oligomers induce an overexpression of Vti1a leading to a high-frequency spontaneous vesicular exocytosis of significant Glu amounts, further accompanied by a downregulation of VGLUT1, ultimately resulting in the depletion of intravesicular Glu content and substantially decreased Glu release, causing neurodegeneration at the late stage of AD; iii) as AD progresses, $A\beta_{42}$ soluble oligomers also affected the fusion pores that allow vesicular release, enlarging their mean radius, hence increasing the fraction of Glu released (Fig. 5*G*). Altogether, these results provide valuable information for understanding the contrasting pathogenic effects induced by $A\beta_{42}$ on Glu synaptic transmission at different AD stages.

Materials and Methods

Materials. SiC nanowires (SiC NWs) were bought from Nanjing/Jiangsu XFNANO Materials Tech Co., Ltd (Nanjing, China). β-Amyloid (1–42) (peptides with 42 amino acid residues) was purchased from ChinaPeptides Co., Ltd (Shanghai, China). DMEM/F-12 medium and B_{27} for cell culture were bought from ThermoFisher scientific Co., Ltd (Shanghai, China). Bovine serum albumin (BSA), polyethyleneimine (PEI), and GluOx were purchased from Sigma-Aldrich Co., Ltd (Shanghai, China). Poly (ethylene glycol) diglycidyl ether (PEGDE) was obtained from Aladdin Industrial Co., Ltd. (Shanghai, China). Nucleic acid purification kit and chemicals for PCR were purchased from TaKaRa Biotechnology Co., Ltd. (Dalian, China).

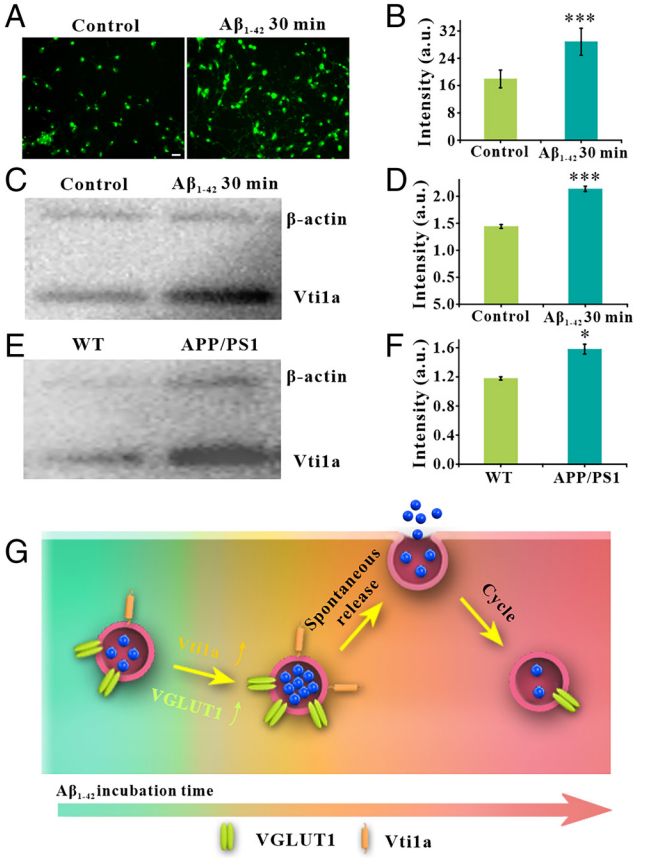

Fig. 5. Influence of $A\beta_{42}$ soluble oligomers on the Vti1a levels in intracellular Glu vesicles in cultured hippocampal neurons exposed to control conditions or incubated with 250 nM $A\beta_{42}$ soluble oligomers during 30 min. (*A*) Representative immunofluorescence images indicating Vti1a levels. (Common scale bar: 20 μm.) (*B*) Relative integrated intensities of Vti1a immunofluorescence levels. (*C*) Western blots of cultured hippocampal neurons exposed to control conditions or incubated with 250 nM $A\beta_{42}$ soluble oligomers during 30 min; β-actin was used as an internal control, and (*D*) plot of the relative densitometric intensities featuring Vti1a levels. (*E*) Western blots of hippocampal area from 2-mo-old WT mice or 2-mo-old APP/PS1 mice, and (*F*) plot of the relative densitometric intensities featuring Vti1a levels. (*G*) Schematic diagram of a possible mechanism rationalizing the observed influence of $A\beta_{42}$ soluble oligomers on vesicular activity. Error is SEM; $^*P < 0.05$, $^{***}P < 0.001$, compared with control.

The probe DNA was received from Sangon Biotech Co., Ltd. (Shanghai, China). Rabbit anti-VGLUT1 was purchased from Abcam Co., Ltd. (Shanghai, China), rabbit anti-Vti1a was bought from Proteintech Co., Ltd. (Wuhan, China), AF488 goat anti-rabbit IgG (H+L) was bought from Jackson Immunoresearch Co., Ltd. (PA, USA), and β-Actin Rabbit mAb (High Dilution) was purchased from ABclonal Co., Ltd. (Wuhan, China). All other chemicals and solvents of analytical grade were obtained from Sinopharm Chemical Reagent Co., Ltd. (Shanghai, China) and used as received unless stated otherwise. When required, all chemical solutions and buffers were prepared in ultrapure water (18.2 MΩ).

Methods.

Hippocampal neuron culture. A suspension of dissociated primary hippocampal neurons was prepared according to published procedures (55). Briefly, the hippocampus was dissected from brain of newborn rat pups at postnatal day 1, followed by digestion with 0.125% trypsin for 30 min at 37 °C, and then the serum-free culture medium was added to terminate the action of the trypsinase. The homogenate was first centrifuged at 2,000 rpm for 10 min. The supernatant was discarded, and the cells were resuspended in DMEM/F-12 supplemented with 2% B27, 100 U/mL penicillin, streptomycin, and 50 ng/mL NGF. The hippocampal neurons were then planted on PLL-coated glass coverslips and cultured at 37 °C under 5% CO_2 in culture medium.

Fabrication of GluOx-modified single nanowire electrodes. GluOx-modified single nanowire electrodes were fabricated according to a previously reported procedure (32). Briefly, SiC@C NWEs' tip was immersed into 1 mM H_2PtCl_6

solution containing 0.2 M Na_2SO_4 for electroplatinization. A large Ag/AgCl wire served as the reference electrode, and cyclic voltammetry was performed (CV scan between −0.5 V and 0 V at a scanning rate of 0.1 V s^{-1}). Then, a droplet of 0.1% w/v PEI solution was first deposited on the platinized area of the SiC@C/Pt NWE and a drop of enzyme solution consisting of 1 mg/mL BSA, 20 U/mL GluOx, and 10 mg/mL PEGDE was then deposited on the platinized area and left to dry at 4 °C overnight in a refrigerator. Electrochemical measurements were carried out on a CHI-660 A electrochemical workstation (CH instruments Inc.) with Ag/AgCl as a reference electrode.

Immunofluorescence. For endogenous protein expression analysis, hippocampal neurons were seeded on PLL-coated glass coverslips for 3 d. Then, cells were washed three times with phosphate-buffered saline solution (PBS) and fixed with ice-cold 4% paraformaldehyde for 15 min at room temperature and subsequently permeabilized with 0.1% of Triton X-100 in PBS for 10 min. After blocking with 1% goat serum, the cells were incubated with the primary antibody (rabbit anti-VGLUT1, rabbit anti-Vti1a antibody) overnight at a temperature of 4 °C. Then, the cells were incubated with a secondary antibody [AF488 goat anti-rabbit IgG (H+L)]. The fluorescence was analyzed using an inverted fluorescent microscope (Axiovert 200 M and AxioObserver Z1, Carl Zeiss).

Western blot analysis. Protein extraction was performed as previously described (30). Briefly, cells (n = 3) and APP/PS1 mouse (n = 3) hippocampal brain tissues were lysed in an ice-cold RIPA lysis buffer (ThermoFisher scientific Co., Ltd, Shanghai, China) supplemented with protease and phosphatase inhibitor cocktail (ThermoFisher scientific Co., Ltd, Shanghai, China). The lysates were centrifuged at 10,000 rpm for 5 min, and the supernatants were collected and stored at −80 °C until analysis. The concentration of total protein was determined using the BCA Protein Assay Kit (ThermoFisher scientific Co., Ltd, Shanghai, China). Equal amounts of protein were electrophoresed in 10% of SDS-PAGE gel, which was then transferred onto a nitrocellulose membrane. The membrane was blocked by incubation with 5% of BSA at room temperature, and then, incubated with the primary antibody (rabbit anti-VGLUT1, rabbit anti-Vti1a antibody, and β-Actin Rabbit mAb) at a temperature of 4 °C overnight, followed by probed with a secondary antibody for detection by chemiluminescence using a WesternBrightTM ECL western blotting detection kit.

PCR, HE staining, and immunohistochemistry (IHC). The DNA was obtained from mouse tail through a commercial nucleic acid purification kit, and the PCR amplification reactions were performed according to published procedures (56).

The hippocampus was obtained and fixed with 4% paraformaldehyde, then embedded and sliced for H&E and IHC staining.

Amperometric measurements, data acquisition, and analysis. All amperometric monitoring experiments were carried out with an inverted microscope (AxioObserver Z1 fluorescence microscope, Zeiss, Germany) coupled to a patch clamp amplifier (EPC-10, HEKA Electronics, Germany). All apparatuses were placed in a Faraday cage and grounded through a common ground. The Glu nanosensor was manufactured as described previously.

Briefly, it was first moved near to the surface of the varicosity membrane of the hippocampal axon neuron with a micromanipulator (TransferMan NK2, Eppendorf, Germany) under the microscope using 100 × objective lens, and then slowly moved forward to penetrate inside the cell for IVIEC measurements or placed laterally on the top of the varicosity for monitoring exocytotic vesicular release spikes with or without high-k^+ solutions (62.5 mM).

The amperometric spikes were recorded by a patchclamp amplifier at a constant potential of +700 mV with Ag/AgCl as reference. Signals were sampled at 10 kHz, and Bessel-filtered at 2.9 kHz. Raw amperometric data were collected using the "Pulse" software and analyzed by Igor Pro software kindly provided by E.V. Mosharov from Columbia University. The threshold criteria for spontaneous exocytotic peak selection were normally five times the SD of the noise of the electrode.

Data, Materials, and Software Availability. All study data are included in the article, *SI Appendix*, and Dryad (https://doi.org/10.5061/dryad.mw6m90621) (57).

ACKNOWLEDGMENTS. W.-H.H., X.-K.Y., X.-K.J., Y.-T.J., X.-W.Z., and Y.-L.L. gratefully acknowledge financial support from the National Natural Science Foundation of China (Grants 21725504, 22090050, 22090051, and 21721005) and the China Postdoctoral Science Foundation (Grants 2022M722456). C.A. gratefully acknowledges the University of Xiamen and its State Key Laboratory of Physical Chemistry of Solid Surfaces (PCOSS, University of Xiamen, China) as well as Paris Sciences Lettre University, École Normale Supérieure, CNRS, and Sorbonne University (UMR 8640). We gratefully acknowledge the Sino-French support of CNRS IRP "NanoBioCatEchem."

Author affiliations: [a]College of Chemistry and Molecular Sciences, Wuhan University, Wuhan 430072, People's Republic of China; [b]State Key Laboratory of Physical Chemistry of Solid Surfaces, College of Chemistry and Chemical Engineering, Xiamen University, Xiamen 361005, People's Republic of China; [c]PASTEUR, Département de Chimie, École Normale Supérieure, Paris Sciences Lettre Research University, Sorbonne University, & University Pierre and Marie Curie, 06 75005 Paris, France; and [d]Department of Hepatobiliary and Pancreatic Surgery, Zhongnan Hospital of Wuhan University, Wuhan 430071, People's Republic of China

1. B. D. Strooper, E. Karran, The cellular phase of Alzheimer's disease. *Cell* **164**, 603–615 (2016).
2. J. J. Palop, L. Mucke, Amyloid-beta-induced neuronal dysfunction in Alzheimer's disease: From synapses toward neural networks. *Nat. Neurosci.* **13**, 812–818 (2010).
3. J. Marschallinger *et al.*, Lipid-droplet-accumulating microglia represent a dysfunctional and proinflammatory state in the aging brain. *Nat. Neurosci.* **23**, 194–208 (2020).
4. J. J. Palop, L. Mucke, Network abnormalities and interneuron dysfunction in Alzheimer disease. *Nat. Rev. Neurosci.* **17**, 777–792 (2016).
5. L. Verret *et al.*, Inhibitory interneuron deficit links altered network activity and cognitive dysfunction in Alzheimer model. *Cell* **149**, 708–721 (2012).
6. C. Lerdkrai *et al.*, Intracellular Ca^{2+} stores control in vivo neuronal hyperactivity in a mouse model of Alzheimer's disease. *Proc. Natl. Acad. Sci. U.S.A.* **115**, E1279–E1288 (2018).
7. D. M. Walsh *et al.*, Naturally secreted oligomers of amyloid β protein potently inhibit hippocampal long-term potentiation in vivo. *Nature* **416**, 535–539 (2002).
8. P. F. Chapman *et al.*, Impaired synaptic plasticity and learning in aged amyloid precursor protein transgenic mice. *Nat. Neurosci.* **2**, 271–276 (1999).
9. R. A. Mitchell, N. Herrmann, K. L. Lanctôt, The role of dopamine in symptoms and treatment of apathy in Alzheimer's disease. *CNS Neurosci. Ther.* **17**, 411–427 (2011).
10. T. H. Ferreira-Vieira, I. M. Guimaraes, F. R. Silva, F. M. Ribeiro, Alzheimer's disease: Targeting the cholinergic system. *Curr. Neuropharmacol.* **14**, 101–115 (2016).
11. Y. Zhou, N. C. Danbolt, Glutamate as a neurotransmitter in the healthy brain. *J. Neural. Transm.* **121**, 799–817 (2014).
12. B. Zott *et al.*, A vicious cycle of β amyloid-dependent neuronal hyperactivation. *Science* **365**, 559–565 (2019).
13. S. Li *et al.*, Soluble oligomers of amyloid beta protein facilitate hippocampal long-term depression by disrupting neuronal glutamate uptake. *Neuron* **62**, 788–801 (2009).
14. M. Talantova *et al.*, Aβ induces astrocytic glutamate release, extrasynaptic NMDA receptor activation, and synaptic loss. *Proc. Natl. Acad. Sci. U.S.A.* **110**, E2518–E2527 (2013).
15. E. Abramov *et al.*, Amyloid-β as a positive endogenous regulator of release probability at hippocampal synapses. *Nat. Neurosci.* **12**, 1567–1576 (2009).
16. C. L. Russell *et al.*, Amyloid-beta acts as a regulator of neurotransmitter release disrupting the interaction between synaptophysin and VAMP2. *PLoS One* **7**, e43201 (2012).
17. Y. Yang *et al.*, Amyloid-β oligomers may impair SNARE-mediated exocytosis by direct binding to syntaxin 1a. *Cell Rep.* **12**, 1244–1251 (2015).
18. N. W. Hu *et al.*, mGlu5 receptors and cellular prion protein mediate amyloid-β-facilitated synaptic long-term depression in vivo. *Nat. Commun.* **5**, 3374 (2014).
19. E. V. Mosharov, D. Sulzer, Analysis of exocytotic events recorded by amperometry. *Nat. Methods* **2**, 651–658 (2005).
20. W. Z. Wu *et al.*, Monitoring dopamine release from single living vesicles with nanoelectrodes. *J. Am. Chem. Soc.* **127**, 8914–8915 (2005).
21. A. Schulte, W. Schuhmann, Single-cell microelectrochemistry. *Angew. Chem. Int. Ed. Engl.* **46**, 8760–8777 (2007).
22. C. Amatore, S. Arbault, M. Guille, F. Lemaître, Electrochemical monitoring of single cell secretion: Vesicular exocytosis and oxidative stress. *Chem. Rev.* **108**, 2585–2621 (2008).
23. M. Ganesana, S. T. Lee, Y. Wang, B. J. Venton, Analytical techniques in neuroscience: Recent advances in imaging, separation, and electrochemical methods. *Anal. Chem.* **89**, 314–341 (2017).
24. N. T. N. Phan, X. Li, A. G. Ewing, Measuring synaptic vesicles using cellular electrochemistry and nanoscale molecular imaging. *Nat. Rev. Chem.* **1**, 0048 (2017).
25. X. Li, S. Majdi, J. Dunevall, H. Fathali, A. G. Ewing, Quantitative measurement of transmitters in individual vesicles in the cytoplasm of single cells with nanotip electrodes. *Angew. Chem. Int. Ed. Engl.* **54**, 11978–11982 (2015).
26. A. Larsson *et al.*, Intracellular electrochemical nanomeasurements reveal that exocytosis of molecules at living neurons is subquantal and complex. *Angew. Chem. Int. Ed. Engl.* **59**, 6711–6714 (2020).
27. Q. F. Qiu *et al.*, Real-time monitoring of exocytotic glutamate release from single neuron by amperometry at an enzymatic biosensor. *Electroanalysis* **30**, 1054–1059 (2018).
28. M. Ganesana, E. Trikantzopoulos, Y. Maniar, S. T. Lee, B. J. Venton, Development of a novel micro biosensor for in vivo monitoring of glutamate release in the brain. *Biosens. Bioelectron.* **130**, 103–109 (2019).
29. Y. Wang *et al.*, Ultrafast glutamate biosensor recordings in brain slices reveal complex single exocytosis transients. *ACS Chem. Neurosci.* **10**, 1744–1752 (2019).
30. X. K. Yang *et al.*, $Aβ_{1-42}$ oligomers induced a short-term increase of glutamate release prior to its depletion as measured by amperometry on single varicosities. *Anal. Chem.* **91**, 15123–15129 (2019).
31. Y. Wang *et al.*, Counting the number of glutamate molecules in single synaptic vesicles. *J. Am. Chem. Soc.* **141**, 17507–17511 (2019).
32. X. K. Yang *et al.*, Quantitative nano-amperometric measurement of intravesicular glutamate content and its sub-quantal release by living neurons. *Angew. Chem. Int. Ed. Engl.* **60**, 15803–15808 (2021).

33. A. Oleinick, I. Svir, C. Amatore, "Full fusionis" not ineluctable during vesicular exocytosis of neurotransmitters by endocrine cells. *Proc. Math. Phys. Eng. Sci.* **473**, 20160684 (2017).
34. E. Marcello *et al.*, Amyloid-β oligomers regulate ADAM10 synaptic localization through aberrant plasticity phenomena. *Mol. Neurobiol.* **56**, 7136–7143 (2019).
35. R. Morkuniene *et al.*, Small $A\beta_{1-42}$ oligomer-induced membrane depolarization of neuronal and microglial cells: Role of N-methyl-D-aspartate receptors. *J. Neurosci. Res.* **93**, 475–486 (2014).
36. D. J. Selkoe, Alzheimer's disease is a synaptic failure. *Science* **298**, 789–791 (2002).
37. S. P. Pallo, J. DiMaio, A. Cook, B. Nilsson, G. V. W. Johnson, Mechanisms of tau and Aβ-induced excitotoxicity. *Brain Res.* **1634**, 119–131 (2016).
38. X. Li, J. Dunevall, A. G. Ewing, Using single-cell amperometry to reveal how cisplatin treatment modulates the release of catecholamine transmitters during exocytosis. *Angew. Chem. Int. Ed. Engl.* **55**, 9041–9044 (2016).
39. L. Ren, A. Oleinick, I. Svir, C. Amatore, A. G. Ewing, Amperometric measurements and dynamic models reveal a mechanism for how zinc alters neurotransmitter release. *Angew. Chem. Int. Ed. Engl.* **59**, 3083–3087 (2020).
40. Y. Wang, C. Gu, A. G. Ewing, Single-vesicle electrochemistry following repetitive stimulation reveals a mechanism for plasticity changes with iron deficiency. *Angew. Chem. Int. Ed. Engl.* **61**, e202200716 (2022).
41. A. Oleinick, F. Lemaître, M. G. Collignon, I. Svir, C. Amatore, Vesicular release of neurotransmitters: Converting amperometric measurements into size, dynamics and energetics of initial fusion pores. *Faraday Discuss.* **164**, 33–55 (2013).
42. J. Lovrić *et al.*, On the mechanism of electrochemical vesicle cytometry: Chromaffin cell vesicles and liposomes. *Faraday Discuss.* **193**, 65–79 (2016).
43. R. Hu *et al.*, How "full" is "full fusion" during exocytosis from dense core vesicles? Effect of SDS on "quantal" release and final fusion pore size. *J. Electrochem. Soc.* **163**, H853–H865 (2016).
44. C. Gu, A. Larsson, A. G. Ewing, Plasticity in exocytosis revealed through the effects of repetitive stimuli affect the content of nanometer vesicles and the fraction of transmitter released. *Proc. Natl. Acad. Sci. U.S.A.* **116**, 21409–21415 (2019).
45. R. W. Daniels *et al.*, A single vesicular glutamate transporter is sufficient to fill a synaptic vesicle. *Neuron* **49**, 11–16 (2006).
46. A. Kashani *et al.*, Loss of VGLUT1 and VGLUT2 in the prefrontal cortex is correlated with cognitive decline in Alzheimer disease. *Neurobiol. Aging* **29**, 1619–1630 (2008).
47. R. T. Fremeau Jr., *et al.*, Vesicular glutamate transporters 1 and 2 target to functionally distinct synaptic release sites. *Science* **304**, 1815–1819 (2004).
48. L. Sheng *et al.*, Microglial Trem2 induces synaptic impairment at early stage and prevents amyloidosis at late stage in APP/PS1 mice. *FASEB J.* **33**, 10425–10442 (2019).
49. P. Fatt, B. Katz, Spontaneous subthreshold activity at motor nerve endings. *J. Physiol.* **117**, 109–128 (1952).
50. J. J. Palop *et al.*, Aberrant excitatory neuronal activity and compensatory remodeling of inhibitory hippocampal circuits in mouse models of Alzheimer's disease. *Neuron* **55**, 697–711 (2007).
51. J. Xu, Z. P. Pang, O. H. Shin, T. C. Südhof, Synaptotagmin-1 functions as a Ca^{2+} sensor for spontaneous release. *Nat. Neurosci.* **12**, 759–766 (2009).
52. A. J. Groffen *et al.*, Doc2b is a high-affinity Ca^{2+} sensor for spontaneous neurotransmitter release. *Science* **327**, 1614–1618 (2010).
53. B. L. Tang, Vesicle transport through interaction with t-SNAREs 1a (Vti1a)'s roles in neurons. *Heliyon* **6**, e04600 (2020).
54. D. M. Ramirez, M. Khvotchev, B. Trauterman, E. T. Kavalali, Vti1a identifies a vesicle pool that preferentially recycles at rest and maintains spontaneous neurotransmission. *Neuron* **73**, 121–134 (2012).
55. S. Kaech, G. Banker, Culturing hippocampal neurons. *Nat. Protoc.* **1**, 2406–2415 (2006).
56. J. H. Yang, B. W. Ju, J. P. Hu, Effects of phenylethanoid glycosides extracted from herba cistanches on the learning and memory of the APP/PSI transgenic mice with Alzheimer's disease. *Biomed. Res. Int.* **2021**, 1291549 (2021).
57. X. K. Yang *et al.*, Nanoelectrochemistry reveals how soluble $A\beta_{42}$ oligomers alter vesicular storage and release of glutamate. *Dryad*. https://doi.org/10.5061/dryad.mw6m90621. Deposited 15 April 2023.